Ecological Informatics 25 (2015) 1–9

Contents lists available at ScienceDirect

Ecological Informatics

journal homepage: www.elsevier.com/locate/ecolinf

Utilization of ground-based digital photography for the evaluation of seasonal changes in the aboveground green biomass and foliage phenology in a grassland ecosystem

Tomoharu Inoue [a,b,*], Shin Nagai [b], Hideki Kobayashi [b], Hiroshi Koizumi [a]

[a] Faculty of Education and Integrated Arts and Sciences, Waseda University, 2-2 Wakamatsu-cho, Shinjuku-ku, Tokyo 162-8480, Japan
[b] Department of Environmental Geochemical Cycle Research, Japan Agency for Marine-Earth Science and Technology (JAMSTEC), 3173-25 Showa-machi, Kanazawa-ku, Yokohama 236-0001, Japan

ARTICLE INFO

Article history:
Received 19 December 2013
Received in revised form 23 September 2014
Accepted 24 September 2014
Available online 13 October 2014

Keywords:
Biomass estimation
Digital camera
Digital repeat photography
Phenological observations
RGB

ABSTRACT

We investigated the usefulness of a ground-based digital photography to evaluate seasonal changes in the aboveground green biomass and foliage phenology in a short-grass grassland in Japan. For ground-truthing purposes, the ecological variables of aboveground green biomass and spectral reflectance of aboveground plant parts were also measured monthly. Seasonal change in a camera-based index (rG: ratio of green channel) reflected the characteristic events of the foliage phenology such as the leaf-flush and leaf senescence. In addition, the seasonal pattern of the rG was similar to that of the aboveground green biomass throughout the year. Moreover, there was a positive linear relationship between rG and aboveground green biomass ($R^2 = 0.81, p < 0.05$), as was the case with spectra-based vegetation indices. On the basis of these results, we conclude that continuous observation using digital cameras is a useful tool that is less labor intensive than conventional methods for estimating aboveground green biomass and monitoring foliage phenology in short-grass grasslands in Japan.

1. Introduction

Grassland ecosystems, which are estimated to cover from 41 to 56 million km^2 or from 31% to 43% of the Earth's land surface, are ranked with forest ecosystems as the main terrestrial ecosystems (Scurlock and Hall, 1998; White et al., 2000). In East Asia, grassland ecosystems are widely distributed in alpine areas and semiarid regions (e.g., the Tibetan and Mongolian Plateaus [Ni, 2002; White et al., 2000; Xiao et al., 1995]). These grasslands provide livelihoods to local residents and serve as carbon sinks and/or sources in the carbon budget (Fang et al., 2007; Ni, 2002; Xiao et al., 1995). However, recent studies have reported that environmental changes such as global warming, overgrazing, and land-use change can alter vegetation and ecosystem functions (e.g., carbon cycle) in these grasslands (Cao et al., 2004; Ma et al., 2010). Because uptake of CO_2 by plants might be the only sustainable way of removing CO_2 from the atmosphere (Eisfelder et al., 2012; Trumper et al., 2008), it is important to conduct quantitative studies of the aboveground plant biomass and the length of the plants' growing seasons in order to predict the response of the carbon cycle to future environmental changes accurately. To achieve these aims, it is necessary to establish techniques for long-term and continuous in situ observations of the spatial and temporal variations in foliage phenology and plant biomass (Eisfelder et al., 2012).

Previous observations of foliage phenology and plant biomass in grasslands fall into two main classes: (1) investigations of a specific area based on conventional ground-based observations, such as clipping and weighing of aboveground plant biomass and direct observations of leaves to detect plant phenological events (e.g., Dhital et al., 2010a,b; Ma et al., 2010; Xiao et al., 1996; Zhang and Skarpe, 1996); and (2) regional or global scale investigations based on satellite remote-sensing observations (e.g., Kawamura et al., 2005; Xu et al., 2008; Yang et al., 2009). Although conventional ground-based observation is the most accurate way to collect biomass data in a fixed area, this approach is both time consuming and labor intensive (Lu, 2006). Therefore, it would be difficult to gather continuous measurements over a wide area using conventional observation techniques (Eisfelder et al., 2012; Ide and Oguma, 2010; Richardson et al., 2009). In contrast, satellite-based monitoring requires little labor and is suitable for the continuous observation of spatial and temporal changes in terrestrial ecosystem structure (e.g., foliage phenology) at regional or global scales (Akiyama and Kawamura, 2007; Eisfelder et al., 2012; Lu, 2006). However, satellite data acquisition is limited by cloud cover and atmospheric conditions (Ide and Oguma, 2010;

* Corresponding author at: Department of Environmental Geochemical Cycle Research, Japan Agency for Marine-Earth Science and Technology (JAMSTEC), 3173-25 Showa-machi, Kanazawa-ku, Yokohama 236-0001, Japan. Tel.: +81 45 778 5614; fax: +81 45 778 5706.
E-mail addresses: tomoharu@aoni.waseda.jp, tomoharu@jamstec.go.jp, tomoharu.inoue.mail@gmail.com (T. Inoue), nagais@jamstec.go.jp (S. Nagai), hkoba@jamstec.go.jp (H. Kobayashi), hkoizumi@waseda.jp (H. Koizumi).

http://dx.doi.org/10.1016/j.ecoinf.2014.09.013
1574-9541/

Muraoka et al., 2012; Nagai et al., 2010). Thus, each approach has its strengths and weaknesses. For continuous, long-term, and accurate evaluations of spatial and temporal variations in ecosystem structure and functions at a large scale, it is important to integrate ground-truthing into the study design, that is, to combine ground-based observations and satellite remote sensing, which allows the scaling-up from a specific area to a regional or global scale (Muraoka et al., 2012).

To bridge the gap between ground-based observations and satellite remote sensing, researchers have begun to focus on near-surface remote-sensing techniques (e.g., Ahrends et al., 2008, 2009; Crimmins and Crimmins, 2008). Among these, most researchers have used the technique that utilizes the red, green, and blue channels of digital numbers (RGBs) extracted from digital repeat photographs taken by tower-mounted digital cameras (e.g., Ide and Oguma, 2010; Nagai et al., 2011; Richardson et al., 2009; Sonnentag et al., 2012). Seasonal changes in vegetation indices calculated from RGBs (camera-based vegetation indices) were closely related to seasonal changes in leaf phenology (i.e., the timing of the leaf-flush and leaf-fall [e.g., Ahrends et al., 2009; Nagai et al., 2011; Richardson et al., 2007]), gross primary production (e.g., Richardson et al., 2009; Saitoh et al., 2012), and the spectral reflectance estimated by a spectroradiometer system (Saitoh et al., 2012). Because digital cameras are relatively inexpensive and easy to use, as compared with other equipments (e.g., spectroradiometer system), they can be used as components of a worldwide network to allow continuous, large-scale, and highly precise monitoring of ecological and environmental variations in an array of ecosystems (Graham et al., 2010; Ide and Oguma, 2010; Nishida, 2007; Richardson et al., 2007). Moreover, such a system can provide ground-truthing of data gathered by satellite remote sensing (Graham et al., 2010; Nagai et al., 2011; Saitoh et al., 2012). However, most previous digital photography studies focused on forest ecosystems (e.g., Ahrends et al., 2009; Richardson et al., 2009; Sonnentag et al., 2012). Few studies have used the digital repeat photography to monitor the temporal variation in grassland structure and function (Migliavacca et al., 2011). Moreover, few such studies have examined the relationship between the plant biomass and the camera data (VanAmburg et al., 2006).

To validate the usefulness of the ground-based digital photography approach in grasslands, we performed 2 years of continuous monitoring with a digital camera and gathered monthly measurements of ecological variables (aboveground green biomass and spectral reflectance of aboveground plant parts) throughout a single year in a short-grass grassland in central Japan. We investigated the relationships between a camera-based vegetation index and these ecological variables. The objectives of this study were (1) to test how well the seasonal changes in each RGB channel obtained from the digital repeat photography or a camera-based vegetation index reflect the temporal variations in ecosystem structure (foliage phenology and aboveground green biomass) in the grassland; and (2) to validate the usefulness of the ground-based digital photography for continuous observations of grassland ecosystems.

2. Methods

2.1. Site description and study period

Our study site is a short-grass grassland located in the central mountain region of Japan (36°08′N, 137°26′E, 1340 m a.s.l.). The grassland is maintained by cattle grazing from May to October. The vegetation consisted primarily of *Zoysia japonica*, but *Ranunculus japonicus* and *Trifolium repens* were also common (Dhital et al., 2010a). The grass height can range from 5 to 10 cm. The annual mean air temperature and annual cumulative precipitation from 1997 to 2006 were 7.2 °C and 2151 mm, respectively (Inoue and Koizumi, 2012). The snow season usually begins in late December and ends in early April. More information about this site is provided by Dhital et al. (2010a,b) and Inoue and Koizumi (2012).

We established a 20 m × 20 m experimental area on a south-facing slope (about 16°) of the study site. The present study was conducted from early May 2010 to early December 2011 (except during the snow season, which extended from late December 2010 to mid-April 2011).

2.2. Observation of foliage phenology using a digital camera system

To observe the foliage phenology, we mounted a digital camera system (Nishida, 2007) on a stand at the site, facing east and providing a view of the whole experimental area. The placement of the system was fixed during the study period. The camera system consisted of a digital camera (Coolpix 4500; Nikon, Tokyo, Japan), a recording controller (SPC31A; Hayasaka Rikoh, Sapporo, Japan), and a lithium-ion battery (Y00-00250, Enax Inc., Tokyo, Japan). Image size was set to 2272 × 1704 pixels. All images were captured with automatic exposure, and the white balance set to "auto." The images were saved in JPEG format. The observation periods were from 6 May (day of year: DOY 126) to 21 December (DOY 355) in 2010 and from 27 April (DOY 117) to 7 December (DOY 341) in 2011. The images were captured at 4-hour intervals between 00:00 and 24:00 h (Japan Standard Time: JST) each day. The timing of the start of leaf-flush (S_{LF}), end of leaf-flush (E_{LF}), start of leaf senescence (S_{LS}), and end of leaf senescence (E_{LS}) was detected by visual inspection of the images. We defined the timings of S_{LF}, E_{LF}, S_{LS}, and E_{LS} as the first day when 10% of leaves had flushed, the first day when 90% of leaves had flushed, the first day when 10% of leaves were withered, and the first day when 90% of leaves were withered, respectively.

2.3. Calculation of the camera-based vegetation indices

We selected one photo that was captured around noon (between 10:30 and 15:30 h JST) per day for the image analysis (see Appendix A for a detailed description). As determined by visual inspection, the images obtained on rainy or foggy days were removed because of noise in the RGB channels. Moreover, some images were also removed from the analysis because of dirt on the camera housing window. In the end, we used 127 and 151 images for the analysis in 2010 and 2011, respectively.

The red, green, and blue channels of digital numbers (DN_R, DN_G, and DN_B, respectively) were extracted from each pixel of an image. We then calculated the averages of DN_R, DN_G, and DN_B within the regions of interest, an example of which is demarcated in white in Fig. 1. These analyses were conducted with the free geographic information system software GRASS GIS (http://grass.osgeo.org). Because both weather conditions (i.e., sunny or cloudy) and solar altitude vary during a day and over each season, the illumination conditions at around noon at the site may not always be equal (Saitoh et al., 2012). To avoid the effects of these variations on the RGBs, we calculated the normalized RGBs (ratios of DN_R, DN_G, and DN_B as percentages of total DN) by using Eqs. (1) to (3). In addition, we used Eq. (4) to calculate the green excess index (GEI), which has been reported as a useful index to evaluate the variation in foliage phenology (e.g., timing of leaf flush) more precisely than the individual RGB channels (Richardson et al., 2007).

$$rR = DN_R/(DN_R + DN_G + DN_B) \quad (1)$$

$$rG = DN_G/(DN_R + DN_G + DN_B) \quad (2)$$

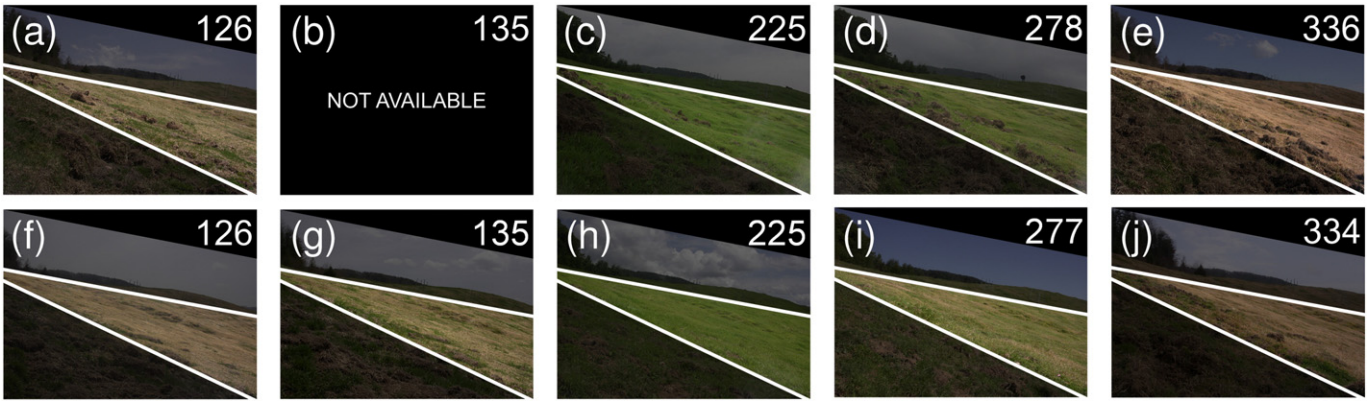

Fig. 1. Typical camera images of the ground surface at the study site in the (a, f) pre-foliation period, (b, g) foliation period, (c, h) leafy period, (d, i) defoliation period, and (e, j) post-defoliation period, in 2010 (a–e) and 2011 (f–j). The number in the upper right of each image is the day of the year on which the picture was taken. Because the camera system was not functioning properly, owing to a dead battery, from DOYs 129 to 149 in 2010, we could not obtain images during the foliation period in 2010. The white outline indicates the region of interest for image analysis. Some parts of the study site (lower left parts of the image) were removed for the image analysis because the areas were dug up by animals during this study period.

$$rB = DN_B/(DN_R + DN_G + DN_B) \quad (3)$$

$$GEI = (DN_G - DN_R) + (DN_G - DN_B) = 2 \times DN_G - (DN_R + DN_B) \quad (4)$$

To record the weather conditions when the camera captured images at the site, we also mounted a camera system (with the same components as noted above) with a fish-eye lens (FC-E8; Nikon) on top of an 18-m-high steel tower erected 700 m north of the site. Images of the sky were captured at 2-min intervals between 06:00 and 17:30 h (JST) each day. We used visual analysis of the images to assess the amount of cloud coverage. We defined the weather conditions as "sunny" when the cloud coverage was 80% or less and as "cloudy" when the cloud coverage was over 80%.

2.4. Observations of the spectral reflectance of the aboveground plant parts

To obtain the spectra-based vegetation indices corresponding to the camera-based vegetation indices, we measured the spectral reflectance of the aboveground plant parts with a portable spectroradiometer (MS-720; Eko Instruments, Tokyo, Japan; spectral range, 350–1050 nm; spectral interval, 3.3 nm; spectral resolution, 10 nm) at monthly intervals from May to December 2011. On each date, we randomly selected six points at the study site. The spectral measurements were performed between 11:00 and 16:00 h (JST). The spectra were measured approximately 25 cm above the ground. The instrument had a field-of-view of 25° and could observe a circular area with a diameter of 11 cm at the ground surface. A 99% diffuse reflectance Spectralon Target (SRT-99-050, Labsphere, Inc., North Sutton, NH, USA) was used to obtain the white reflectance. We calculated the spectral reflectance as the ratio for the reflectance of the target.

2.5. Calculation of spectra-based vegetation indices

Using the above-mentioned spectral data, we calculated spectra-based vegetation indices. Because previous studies reported that the normalized difference vegetation index (NDVI), green normalized difference vegetation index (GNDVI), ratio vegetation index (RVI), difference vegetation index (DVI), and enhanced vegetation index (EVI) were correlated with aboveground plant biomass in grasslands (Chen et al., 2009; Itano and Tomimatsu, 2011; Itano et al., 2000), we calculated these vegetation indices by using Eqs. (5) to (9):

$$NDVI = (NIR_{ave} - red_{ave})/(NIR_{ave} + red_{ave}) \quad (5)$$

$$GNDVI = (NIR_{ave} - green_{ave})/(NIR_{ave} + green_{ave}) \quad (6)$$

$$RVI = R_a/R_b \quad (7)$$

$$DVI = NIR_{ave} - red_{ave} \quad (8)$$

$$EVI = G \times \{(NIR_{ave} - red_{ave})/[NIR_{ave} + (C_1 \times red_{ave}) - (C_2 \times blue_{ave}) + L]\}. \quad (9)$$

On the basis of the Moderate Resolution Imaging Spectroradiometer (MODIS) sensor specifications (http://modis.gsfc.nasa.gov), we used the average value of the spectral data from 620 to 670 nm, 545 to 565 nm, 459 to 479 nm, and 841 to 876 nm as the reflectance in the red_{ave}, $green_{ave}$, $blue_{ave}$, and NIR_{ave} (NIR: near infra-red) bands, respectively, and the data of 770 and 485 nm as the reflectance in the R_a and R_b bands, respectively (Itano and Tomimatsu, 2011). $G = 2.5$, $C_1 = 6$, $C_2 = 7.5$, and $L = 1$ are constants (Huete et al., 2002). Moreover, we also calculated spectra-based rG (rG_Sp), and spectra-based GEI (GEI_Sp) by substituting red_{ave}, $green_{ave}$, and $blue_{ave}$ for DN_R, DN_G, and DN_B into Eqs. (2) and (4), respectively (Saitoh et al., 2012). Correlations of aboveground green biomass with each spectra-based vegetation index were evaluated.

2.6. Measurements of aboveground green biomass

During each spectral reflectance measurement, we also measured aboveground green biomass. Five circular areas with a diameter of 11 cm at the ground surface were randomly selected at the site. The aboveground plant parts inside the area were clipped at the soil surface and collected. These field measurements were conducted monthly from May to November 2011, with the circular area selected at different points each month. The collected aboveground plant parts were sorted into *Z. japonica*, other grasses, and senescent leaves. The green aboveground green biomass of *Z. japonica* and other grasses was then

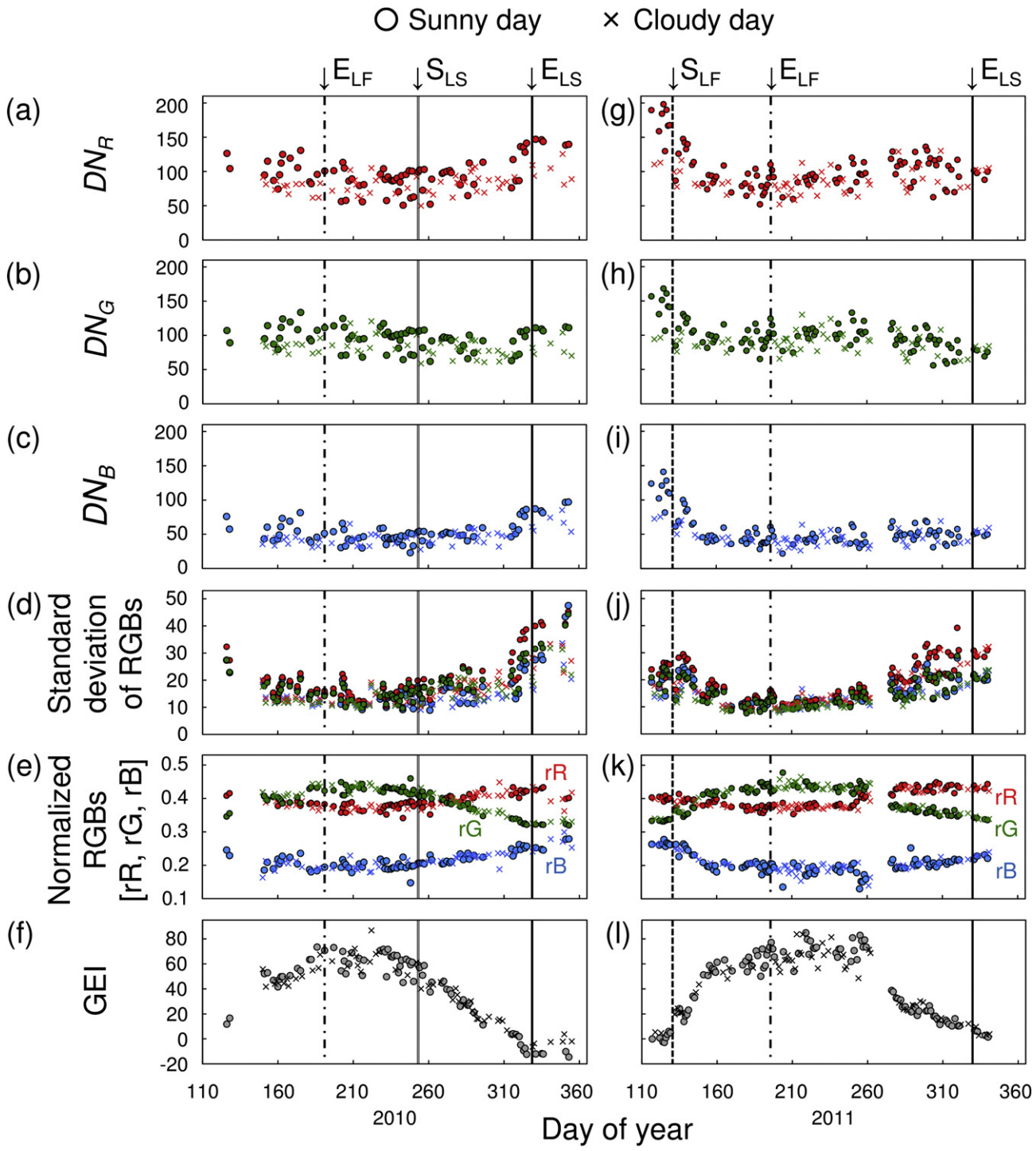

Fig. 2. Seasonal changes in (a, g) DN_R, (b, h) DN_G, (c, i) DN_B, (d, j) standard deviation of RGBs, (e, k) normalized RGBs (rR, rG, and rB), and (f, l) green excess index (GEI) during 2010 (a–f) and 2011 (g–l). Circles and crosses indicate that the weather condition when the camera captured the image was sunny and cloudy, respectively. Red, green, blue, and gray symbols indicate DN_R, DN_G, DN_B, and GEI respectively. Vertical lines indicate the timing of start of leaf-flush (S_{LF}), end of leaf-flush (E_{LF}), start of leaf senescence (S_{LS}), and end of leaf senescence (E_{LS}).

separately oven-dried at 70 °C for 48 h and weighed. Finally, we calculated the average aboveground green biomass for each month.

3. Results

3.1. Seasonal changes in RGB channels and camera-based vegetation index

Typical camera images of the ground surface at the study site are shown in Fig. 1. The average value of DN_R, DN_G, and DN_B, and the standard deviation of RGBs during the study periods are shown in Fig. 2. Because the camera system was not functioning properly because of a dead battery from DOYs 129 to 149 (early May to late May) in 2010 and from DOYs 263 to 275 (late September to early October) in 2011, we could not obtain the RGB channels during these periods.

In 2010, DN_R and DN_B decreased slightly from DOYs 126 to 260 (May to September). After that, the values increased from DOYs 315 to 355 (November to December; Fig. 2a,c). In contrast, DN_G did not show

remarkable seasonal changes (Fig. 2b). The standard deviation of RGBs showed a broad range from DOYs 260 to 355 (September to December; Fig. 2d).

In 2011, the DN_R decreased from DOYs 117 to 170 (April to June), and then it gradually increased until DOY 300 (October; Fig. 2g). After that it decreased again in December. The DN_G also decreased from DOYs 117 to 170, and then it increased from DOYs 170 to 250 (June to September; Fig. 2h). After that it gradually decreased again from DOYs 250 to 320 (September to November). In contrast, the DN_B showed little seasonal changes from DOYs 170 to 341 (June to December; Fig. 2i). The standard deviation of RGBs showed large ranges during two time periods: DOY 117 to 160 and DOY 276 to 341 (Fig. 2j).

The fluctuations of the seasonal changes in each RGB channel were reduced by normalization (Fig. 2e,k). In 2010, although the RGBs were lacking during mid-May, the rG increased from DOYs 126 to 150 (early May to late May) and it reached the maximum level from DOYs 183 to 260 (early July to mid-September). From DOYs 260 to 355 (mid-September to mid-December), the rG gradually decreased and reached the minimum level. In contrast, the rR and rB gradually decreased from DOYs 126 to 215 (May to August), and then they gradually increased from DOYs 215 to 336 (August to December).

In 2011, the values of rG from DOYs 117 to 129 (late April to early May) were almost constant (0.33–0.34). After that, rG began to increase from DOYs 132 to 151 (mid-May to late May) and it reached the maximum level around DOY 200 (July). From DOYs 262 to 276 (late September to early October), the rG decreased rapidly. After that, it gradually decreased and reached the minimum level on DOY 340 (December). In contrast, the rR gradually decreased from DOYs 122 to 170 (May to June), rapidly increased from DOYs 250 to 280 (September to October), and then remained nearly constant until DOY 341. The rB gradually decreased until DOY 200, and then it gradually increased until DOY 341.

The GEI had a bell-shaped seasonal pattern similar to that of the rG during the two years (Fig. 2f,l). In 2011, the values of GEI were nearly zero (from −3 to 6) between DOYs 117 and 129 (early May), and it increased rapidly from DOYs 132 to 200 (mid-May to July), reaching about 70. Although the GEI peaked around 85 for a short time, it generally remained about 70 from DOYs 200 to 262 (July to September). After September, it gradually decreased and was nearly zero on DOY 340. A similar seasonal variation in GEI was observed in 2010, although it began to decrease gradually from DOY 240 (late August).

The RGBs on sunny days were higher than those on cloudy days (Fig. 2a–c,g–i). However, these fluctuations were reduced by normalization (Fig. 2e,k).

3.2. Seasonal changes in spectra-based vegetation indices

All the spectra-based vegetation indices calculated in this study reached the maximum level on DOY 228 (mid-August) (Fig. 3). Both NDVI and GNDVI showed a bell-shaped seasonal pattern, whereas the seasonal pattern of RVI, DVI, and EVI had a distinct peak. Moreover, NDVI and GNDVI varied among measurement spots on DOYs 136 (mid-May), 290 (mid-October), 317 (mid-November), and 341 (early December), but there was less spatial variation on DOYs 170 (mid-June), 205 (late-July), 228 (mid-August), and 255 (mid-September). In contrast, RVI, DVI, and EVI showed large spatial variations during the entire measurement period.

3.3. Seasonal changes in foliage phenology and aboveground green biomass

Visual analysis of the foliage images in 2011 (data not shown) showed that leaf flush of grasses started on DOY 130 (early May) and was nearly finished by DOY 196 (mid-July). During the leaf-flushing period, the study site was dotted with leafless and leafed areas because the timing of foliation was uneven across the site (see Fig. 1g). From DOYs 196 to 262 (mid-July to mid-September), the leaves remained unchanged in appearance. Leaves had already begun to wither on DOY 276 (early October), and senescence was almost complete on DOY 331 (late November). In 2010, we could not evaluate the timing of the start of leaf flush

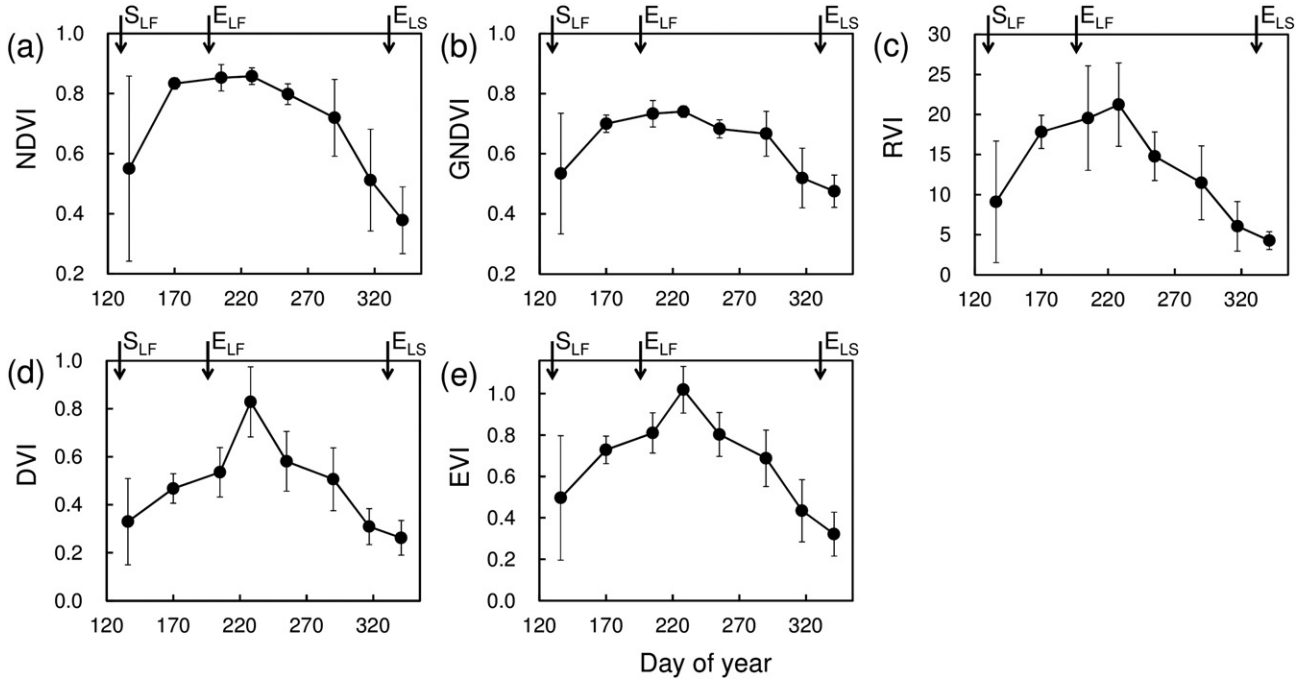

Fig. 3. Seasonal changes in (a) NDVI, (b) GNDVI, (c) RVI, (d) DVI, and (e) EVI in 2011. Error bars indicate the standard deviation. Arrows indicate the timing of the start of leaf-flush (S_{LF}), end of leaf-flush (E_{LF}), and end of leaf senescence (E_{LS}).

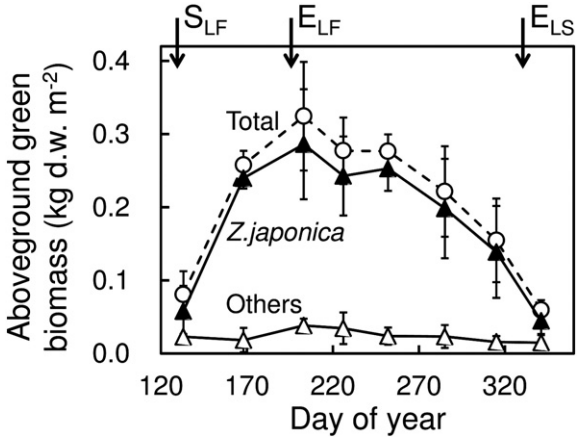

Fig. 4. Seasonal changes in aboveground green biomass in 2011. Error bars indicate the standard deviation. Arrows indicate the timing of the start of leaf-flush (S_{LF}), end of leaf-flush (E_{LF}), and end of leaf senescence (E_{LS}). "d.w." is an abbreviation for "dry weight".

because of a lack of images. The leaf flush was nearly finished by DOY 191 (mid-July). Leaves began to wither on DOY 254 (mid-September) and senescence was complete on DOY 329 (late November).

In 2011, the total aboveground green biomass showed a seasonal pattern (Fig. 4) similar to those of the camera-based indices (rG and GEI). The aboveground green biomass was 0.08 kg d.w. m^{-2} soon after the start of leaf-flush (DOY 133), and then it increased to 0.26 kg d.w. m^{-2} on DOY 168 (mid-June). In late July (DOY 203), it reached the maximum level of 0.32 kg d.w. m^{-2}. After September, it gradually decreased and reached the minimum of 0.06 kg d.w. m^{-2} on DOY 341 (early December). The ratio of aboveground *Z. japonica* biomass to total aboveground green biomass was about 90% from DOYs 168 to 315, whereas it accounted for 72% and 75% in May (DOY 133) and December (DOY 341), respectively.

3.4. Relationships between the vegetation indices and aboveground green biomass

There were significant positive linear relationships between vegetation indices (rG, GEI, and spectra-based vegetation indices) and aboveground green biomass (Fig. 5). The rG and rG_Sp were more strongly correlated with seasonal changes in aboveground green biomass ($R^2 = 0.81$ and 0.82, respectively; $p < 0.05$) than were GEI, GEI_Sp, and DVI ($R^2 = 0.73$, 0.66, and 0.61, respectively; $p < 0.05$), but the coefficients of determination for rG and rG_Sp were smaller than those of NDVI and GNDVI ($R^2 = 0.90$ and 0.91, respectively; $p < 0.05$). The coefficients of determination for RVI and EVI were similar to that of rG ($R^2 = 0.79$ and 0.78, respectively; $p < 0.05$).

4. Discussion

4.1. Evaluation of temporal variations in foliage phenology using the camera-based vegetation index

The start date of leaf-flush at this site in 2011 estimated by the visual analysis of the images (estimated date: DOY 130) agreed well with the timing based on an increase in GEI and rG (DOY 132). In addition, the timings of E_{LF} and E_{LS} detected by the visual analysis corresponded to the maximum and minimum levels of GEI and rG, respectively. Moreover, both the decrease of GEI and rG and the increase of rR were shown more clearly after the timing of S_{LS} detected by the visual analysis. In this way, seasonal changes in the camera-based indices reflected the characteristic events of the foliage phenology at this site. Previous reports on the seasonal changes in these camera-based indices in forest sites (Ide and Oguma, 2010; Nagai et al., 2011; Richardson et al., 2009; Saitoh et al., 2012) noted a marked spike in the GEI after the leaf-flush period, which we did not observe in the grassland (Fig. 2e,f, k,l), although the GEI in both forest and grassland sites showed a bell-shaped seasonal pattern. However, the seasonal pattern of GEI at our site agreed with previous research conducted at a subalpine grassland (Migliavacca et al., 2011). This difference in the seasonal patterns of GEI between forest and grassland sites might reflect differences in the leaf growth characteristics between the two types of

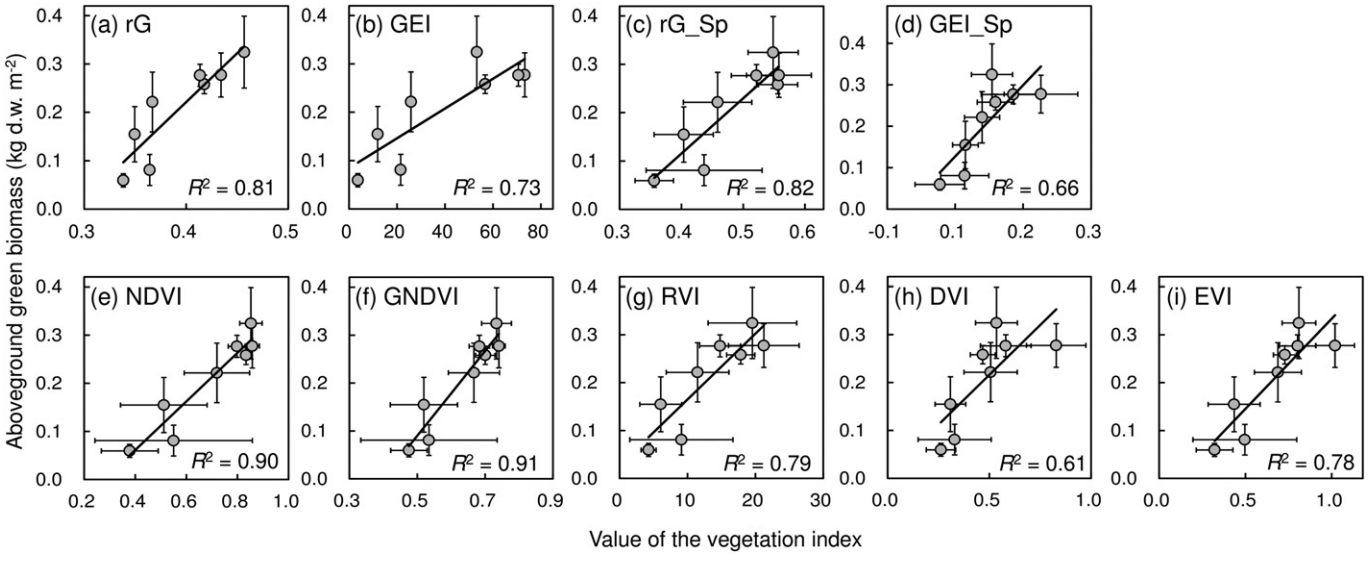

Fig. 5. Relationships between the camera-based and spectra-based vegetation indices (rG, rG_Sp, GEI, GEI_Sp, NDVI, GNDVI, RVI, DVI, and EVI) and the aboveground green biomass. "d.w." is an abbreviation for "dry weight". Error bars indicate the standard deviation. The black solid line represents the regression line for each vegetation index. We selected the camera-based vegetation indices of the day when the aboveground green biomass was collected. If we could not obtain the images because of rain or fog on the day when the material was collected, the image taken on the previous day was used.

ecosystems. In a deciduous forest site, Nagai et al. (2011) noted that the increase of photosynthetic pigments related to the increasing or decreasing of rR and rG occurred later than the leaf area increase. However, photosynthetic pigmentation and leaf area increased simultaneously in a grassland site (Nishida and Higuchi, 2000). Moreover, we found that the range of the standard deviation of RGBs in summer 2011 was smaller than that in summer 2010, which suggests that leaf growth occurred simultaneously within all grasses at the site in 2011. This result also suggests that the standard deviation of RGBs may be a useful index for observing the interannual variation in differences of foliage phenology among the grasses at the site.

Our results indicate that the continuous observation of foliage phenology, which requires much labor if conducted by using conventional ground-based observation techniques, can be achieved in a much simpler manner by using digital cameras, as noted by Ide and Oguma (2010). However, researchers must be aware that the color balance of camera images can change over time (Ide and Oguma, 2010) and there may be a difference in camera-based indices among various digital camera models (Sonnentag et al., 2012). Thus, a standardized and consistent calibration method is required for the establishment of long-term observation with this technique across different sites with different digital cameras.

Use of the threshold value of the camera-based vegetation index is one of the useful approaches for automatic detection of the phenological events such as leaf-flush (Nagai et al., 2013). Inoue et al. (2014) statistically evaluated the suitable threshold value of GEI for detection of the timings of start of leaf-flush and end of leaf-fall in a deciduous broad-leaved forest in Japan by using daily canopy surface photographs over 10 years. As is the case with Inoue et al. (2014), long-term camera monitoring is required to evaluate the suitable threshold value of the camera-based vegetation index for automatic detection of the phenological timings in this study site.

4.2. Relationships between aboveground green biomass and spectra- and camera-based vegetation indices

The rG and GEI showed a positive linear relationship with aboveground green biomass (Fig. 5a,b), as did the spectra-based vegetation indices (Fig. 5c–i), similar to previous studies that reported the relationship between the spectra-based vegetation index and aboveground green biomass in grasslands (Itano and Tomimatsu, 2011). However, the R^2 values varied widely among the spectra-based vegetation indices (from 0.61 to 0.91). The spectral reflectance of the aboveground plant parts obtained by hyperspectral sensor measurements could represent variation in both the leaf forms of different species and the photosynthetic pigment content in the leaves. For example, the reflection of NIR could capture seasonal changes in leaf form (e.g., leaf area [Justice et al., 1985]), and the reflection of both red and green represents the seasonal changes in leaf color indicating changes in the amounts of specific pigments (i.e., anthocyanin and chlorophyll [Sims and Gamon, 2002]). These findings highlight the importance of selecting the spectra-based vegetation index that uses the optimum spectral band at a study site when estimating aboveground green biomass based on a spectra-based vegetation index (Chen et al., 2009; Itano and Tomimatsu, 2011). Our results suggest that a spectroradiometer should provide high-quality data for estimating the aboveground green biomass (e.g., Fig. 5 shows that NDVI and GNDVI had the highest R^2 values). However, continuous spectral measurement is very costly. In contrast, a digital camera system can obtain near-surface remote-sensing images continuously, yet inexpensively. Its radiometric quality is not as good as that of a spectroradiometer, but a digital camera system is inexpensive and much less labor-intensive to use, while providing aboveground green biomass estimates as good as those obtained with a spectroradiometer (relationship between rG and aboveground green biomass: $R^2 = 0.81$).

5. Conclusion

Aboveground green biomass and the length of the plants' growing seasons are important ecological information for understanding the response of the carbon cycle to future environmental changes. However, direct observation methods are too labor intensive to be suitable for continuous long-term observations. In this study, we tested whether a ground-based digital photography is suitable for the continuous evaluation of seasonal changes in aboveground green biomass and foliage phenology in a short-grass grassland of Japan. Image analysis indicated that seasonal variation in the camera-based vegetation index (rG: ratio of green channel) reflected the characteristic events of the foliage phenology such as the leaf-flush and leaf senescence and corresponded well with seasonal variation in aboveground green biomass. Although we did not make long-term measurements, our results suggest the feasibility of using a digital camera system for continuous long-term monitoring of foliage phenology and estimation of aboveground green biomass in short-grass grasslands in Japan, in a manner that is less labor intensive than the use of convention methods. Our future research will be focused on the clarification of the generality of this approach. We need to test whether this approach is suitable for the continuous evaluation of seasonal changes in aboveground green biomass and foliage phenology in various types of grasslands.

Acknowledgments

We thank K. Kurumado and Y. Miyamoto (Takayama Field Station of River Basin Research Center, Gifu University) and M. Ozaki (Waseda University) for their assistance in our field observations. We also thank all Phenological Eyes Network members for their cooperation. We would like to appreciate the reviewer's comments which helped improve this paper. Financial support for this study was provided by the Japan Society for the Promotion of Science (JSPS)/National Research Foundation of Korea (NRF)/National Natural Science Foundation of China (NSFC) A3 Foresight Program (Gifu University, Korea University, and Peking University). H. Kobayashi, S. Nagai, and T. Inoue were supported by KAKENHI (25281014; Grant-in-Aid for Scientific Research B by JSPS). T. Inoue was supported by the Waseda University Grant for Special Research Projects (project nos. 2011A-841, 2012B-053, and 2013A-6166). T. Inoue and S. Nagai were also supported by the Environment Research and Technology Development Fund (S-9) of the Ministry of the Environment of Japan.

Appendix A

To investigate the effect of the diurnal changes in solar altitude on the RGBs, we examined the seasonal changes in the differences between the value of RGB channels at 4 h before noon (i.e., morning) and 4 h after noon (afternoon) as compared to the value around noon (Fig. A1). We found that the RGB channels obtained during the morning tended to be lower than those around noon throughout the year, whereas values obtained during the afternoon tended to be higher than those around noon. These results suggested that the illumination effect on the RGBs in the noon tended to be lower than that in the morning and afternoon. Therefore, to avoid the effects of diurnal changes in solar altitude on the RGBs, we used the images captured around noon in our analysis.

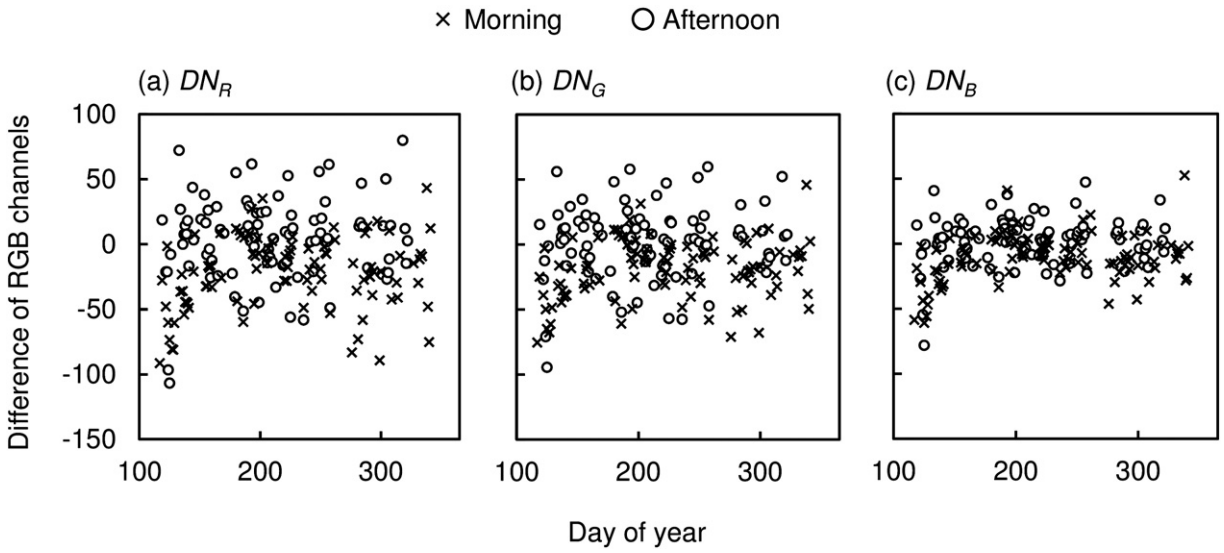

Fig. A1. Seasonal changes in the difference between the morning and afternoon values of the RGB channels as compared to those around noon in 2011.

References

Ahrends, H.E., Brügger, R., Stöckli, R., Schenk, J., Michna, P., Jeanneret, F., Wanner, H., Eugster, W., 2008. Quantitative phenological observations of a mixed beech forest in northern Switzerland with digital photography. J. Geophys. Res. Biogeosci. 113, G04004. http://dx.doi.org/10.1029/2007JG000650.

Ahrends, H.E., Etzold, S., Kutsch, W.L., Stoeckli, R., Bruegger, R., Jeanneret, F., Wanner, H., Buchmann, N., Eugster, W., 2009. Tree phenology and carbon dioxide fluxes: use of digital photography for process-based interpretation at the ecosystem scale. Clim. Res. 39 (3), 261–274.

Akiyama, T., Kawamura, K., 2007. Grassland degradation in China: methods of monitoring, management and restoration. Grassl. Sci. 53 (1), 1–17.

Cao, G.M., Tang, Y.H., Mo, W.H., Wang, Y.A., Li, Y.N., Zhao, X.Q., 2004. Grazing intensity alters soil respiration in an alpine meadow on the Tibetan plateau. Soil Biol. Biochem. 36 (2), 237–243.

Chen, J., Gu, S., Shen, M., Tang, Y., Matsushita, B., 2009. Estimating aboveground biomass of grassland having a high canopy cover: an exploratory analysis of in situ hyperspectral data. Int. J. Remote Sens. 30 (24), 6497–6517.

Crimmins, M.A., Crimmins, T.M., 2008. Monitoring plant phenology using digital repeat photography. Environ. Manage. 41, 949–958.

Dhital, D., Muraoka, H., Yashiro, Y., Shizu, Y., Koizumi, H., 2010a. Measurement of net ecosystem production and ecosystem respiration in a *Zoysia japonica* grassland, central Japan, by the chamber method. Ecol. Res. 25 (2), 483–493.

Dhital, D., Yashiro, Y., Ohtsuka, T., Noda, H., Shizu, Y., Koizumi, H., 2010b. Carbon dynamics and budget in a *Zoysia japonica* grassland, central Japan. J. Plant Res. 123 (4), 519–530.

Eisfelder, C., Kuenzer, C., Dech, S., 2012. Derivation of biomass information for semi-arid areas using remote-sensing data. Int. J. Remote Sens. 33 (9), 2937–2984.

Fang, J.Y., Guo, Z.D., Piao, S.L., Chen, A.P., 2007. Terrestrial vegetation carbon sinks in China, 1981–2000. Sci. China. Ser. D Earth Sci. 50 (9), 1341–1350.

Graham, E.A., Riordan, E.C., Yuen, E.M., Estrin, D., Rundel, P.W., 2010. Public internet-connected cameras used as a cross-continental ground-based plant phenology monitoring system. Glob. Chang. Biol. 16 (11), 3014–3023.

Huete, A., Didan, K., Miura, T., Rodriguez, E.P., Gao, W., Ferreira, L.G., 2002. Overview of the radiometric and biophysical performance of the MODIS vegetation indices. Remote Sens. Environ. 83, 195–213.

Ide, R., Oguma, H., 2010. Use of digital cameras for phenological observations. Ecol. Inform. 5, 339–347.

Inoue, T., Koizumi, H., 2012. Effects of environmental factors upon variation in soil respiration of a *Zoysia japonica* grassland, central Japan. Ecol. Res. 27, 445–452.

Inoue, T., Nagai, S., Saitoh, T.M., Muraoka, H., Nasahara, K.N., Koizumi, H., 2014. Detection of the different characteristics of year-to-year variation in foliage phenology among deciduous broad-leaved tree species by using daily continuous canopy surface images. Ecol. Inform. 22, 58–68. http://dx.doi.org/10.1016/j.ecoinf.2014.05.009.

Itano, S., Tomimatsu, H., 2011. Reflectance spectra for monitoring green herbage mass in *Zoysia*-dominated pastures. Grassl. Sci. 57 (1), 9–17.

Itano, S., Akiyama, T., Ishida, H., Okubo, T., Watanabe, N., 2000. Spectral characteristics of aboveground biomass, plant coverage, and plant height in Italian ryegrass (*Lolium multiflorum* L.) meadows. Grassl. Sci. 46 (1), 1–9.

Justice, C.O., Townshend, J.R.G., Holben, B.N., Tucker, C.J., 1985. Analysis of the phenology of global vegetation using meteorological satellite data. Int. J. Remote Sens. 6 (8), 1271–1318.

Kawamura, K., Akiyama, T., Yokota, H., Tsutsumi, M., Yasuda, T., Watanabe, O., Wang, G., Wang, S., 2005. Monitoring of forage conditions with MODIS imagery in the Xilingol steppe, Inner Mongolia. Int. J. Remote Sens. 26 (7), 1423–1436.

Lu, D.S., 2006. The potential and challenge of remote sensing-based biomass estimation. Int. J. Remote Sens. 27 (7), 1297–1328.

Ma, W.H., Liu, Z.L., Wang, Z.H., Wang, W., Liang, C.Z., Tang, Y.H., He, J.S., Fang, J.F., 2010. Climate change alters interannual variation of grassland aboveground productivity: evidence from a 22-year measurement series in the Inner Mongolian grassland. J. Plant Res. 124 (4), 509–517.

Migliavacca, M., Galvagno, M., Cremonese, E., Rossini, M., Meroni, M., Sonnentag, O., Cogliati, S., Manca, G., Diotri, F., Busetto, L., Cescatti, A., Colombo, R., Fava, F., Morra di Cella, U., Pari, E., Siniscalco, C., Richardson, A.D., 2011. Using digital repeat photography and eddy covariance data to model grassland phenology and photosynthetic CO_2 uptake. Agric. For. Meteorol. 151, 1325–1337.

Muraoka, H., Ishii, R., Nagai, S., Suzuki, R., Motohka, T., Noda, H., Hirota, M., Nasahara, K.N., Oguma, H., Muramatsu, K., 2012. Linking remote sensing and in situ ecosystem/biodiversity observations by "satellite ecology". In: Nakano, S., Nakashizuka, T., Yahara, T. (Eds.), Biodiversity Observation Network in the Asia-Pacific Region. Springer Verlag, Tokyo, Japan, pp. 277–308.

Nagai, S., Nasahara, K.N., Muraoka, H., Akiyama, T., Tsuchida, S., 2010. Field experiments to test the use of the normalized-difference vegetation index for phenology detection. Agric. For. Meteorol. 150 (2), 152–160.

Nagai, S., Maeda, T., Gamo, M., Muraoka, H., Suzuki, R., Nasahara, K.N., 2011. Using digital camera images to detect canopy condition of deciduous broad-leaved trees. Plant Ecolog. Divers. 4 (1), 79–89.

Nagai, S., Saitoh, T.M., Kurumado, K., Tamagawa, I., Kobayashi, H., Inoue, T., Suzuki, R., Gamo, M., Muraoka, H., Nasahara, K.N., 2013. Detection of bio-meteorological year-to-year variation by using digital canopy surface images of a deciduous broad-leaved forest. SOLA 9, 106–110. http://dx.doi.org/10.2151/sola.2013-024.

Ni, J., 2002. Carbon storage in grasslands of China. J. Arid Environ. 50 (2), 205–218.

Nishida, K., 2007. Phenological Eyes Network (PEN): a validation network for remote sensing of the terrestrial ecosystems. AsiaFlux Newsl. 21, 9–13 (available online at http://www.asiaflux.net/newsletter.html).

Nishida, K.N., Higuchi, A., 2000. Seasonal change of grassland vegetation found in the preliminary GLI experiment in the environmental research center. Bull. Terr. Environ. Res. Center, Tsukuba Univ. 1, 1–10 (in Japanese with English summary).

Richardson, A.D., Jenkins, J.P., Braswell, B.H., Hollinger, D.Y., Ollinger, S.V., Smith, M.L., 2007. Use of digital webcam images to track spring green-up in a deciduous broadleaf forest. Oecologia 152 (2), 323–334.

Richardson, A.D., Braswell, B.H., Hollinger, D.Y., Jenkins, J.P., Ollinger, S.V., 2009. Near-surface remote sensing of spatial and temporal variation in canopy phenology. Ecol. Appl. 19 (6), 1417–1428.

Saitoh, T.M., Nagai, S., Saigusa, N., Kobayashi, H., Suzuki, R., Nasahara, K.N., Muraoka, H., 2012. Assessing the use of camera-based indices for characterizing canopy phenology in relation to gross primary production in a deciduous broad-leaved and an evergreen coniferous forest in Japan. Ecol. Inform. 11, 45–54.

Scurlock, J.M.O., Hall, D.O., 1998. The global carbon sink: a grassland perspective. Glob. Chang. Biol. 4 (2), 229–233.

Sims, D.A., Gamon, J.A., 2002. Relationships between leaf pigment content and spectral reflectance across a wide range of species, leaf structures and developmental stages. Remote Sens. Environ. 81, 337–354.

Sonnentag, O., Hufkens, K., Teshera-Sterne, C., Young, A.M., Friedl, M., Braswell, B.H., Milliman, T., O'Keefe, J., Richardson, A.D., 2012. Digital repeat photography for phenological research in forest ecosystems. Agric. For. Meteorol. 152, 159–177.

Trumper, K., Ravilious, C., Dickson, B., 2008. Carbon in drylands: desertification, climate change and carbon finance. UNEP-WCMC (United Nations Environment Programme World Conservation Monitoring Centre), (available online at http://www.unep-wcmc.org/carbon-in-drylands-desertification-climate-change-and-carbon-finance_197.html).

VanAmburg, L.K., Trlica, M.J., Hoffer, R.M., Weltz, M.A., 2006. Ground based digital imagery for grassland biomass estimation. Int. J. Remote Sens. 27 (5), 939–950.

White, R.P., Murray, S., Rohweder, M., 2000. Pilot Analysis of Global Ecosystems: Grassland Ecosystems. World Resources Institute, Washington D.C., USA.
Xiao, X., Ojima, D.S., Parton, W.J., Chen, Z., Chen, D., 1995. Sensitivity of Inner Mongolia grasslands to climate change. J. Biogeogr. 22, 643–648.
Xiao, X.M., Shu, J., Wang, Y.F., Ojima, D.S., Bonham, C.D., 1996. Temporal variation in aboveground biomass of *Leymus chinense* steppe from species to community levels in the Xilin River Basin, Inner Mongolia, China. Vegetatio 123 (1), 1–12.
Xu, B., Yang, X.C., Tao, W.G., Qin, Z.H., Liu, H.Q., Miao, J.M., Bi, Y.Y., 2008. MODIS-based remote sensing monitoring of grass production in China. Int. J. Remote Sens. 29 (17/18), 5313–5327.
Yang, Y.H., Fang, J.Y., Pan, Y.D., Ji, C.J., 2009. Aboveground biomass in Tibetan grasslands. J. Arid Environ. 73 (1), 91–95.
Zhang, W., Skarpe, C., 1996. Small-scale vegetation dynamics in semi-arid steppe in Inner Mongolia. J. Arid Environ. 34 (4), 421–439.